
PNNCLR: STOCHASTIC PSEUDO NEIGHBORHOODS FOR CONTRASTIVE LEARNING BASED UNSUPERVISED REPRESENTATION LEARNING PROBLEMS

Momojit Biswas
Jadavpur University
Kolkata, India
mb16biswas@gmail.com

Himanshu Buckchash
UiT The Arctic University of Norway
Tromsø, Norway
himanshu.buckchash@uit.no

Dilip K. Prasad
UiT The Arctic University of Norway
Tromsø, Norway
dilip.prasad@uit.no

ABSTRACT

Nearest neighbor (NN) sampling provides more semantic variations than pre-defined transformations for self-supervised learning (SSL) based image recognition problems. However, its performance is restricted by the quality of the support set, which holds positive samples for the contrastive loss. In this work, we show that the quality of the support set plays a crucial role in any nearest neighbor based method for SSL. We then provide a refined baseline (pNNCLR) to the nearest neighbor based SSL approach (NNCLR). To this end, we introduce pseudo nearest neighbors (pNN) to control the quality of the support set, wherein, rather than sampling the nearest neighbors, we sample in the vicinity of hard nearest neighbors by varying the magnitude of the resultant vector and employing a stochastic sampling strategy to improve the performance. Additionally, to stabilize the effects of uncertainty in NN-based learning, we employ a smooth-weight-update approach for training the proposed network. Evaluation of the proposed method on multiple public image recognition and medical image recognition datasets shows that it performs up to 8 percent better than the baseline nearest neighbor method, and is comparable to other previously proposed SSL methods.

Keywords self supervised learning · image classification · contrastive learning · pseudo nearest neighbors

1 Introduction

Deep learning is rapidly revolutionizing almost every sector of our society. Off-the-shelf models are being used for feature/representation extraction, and standard models are being fine-tuned for their application to specific problems [1]. To train such models, efficient representation learning methods are required [2]. SSL or representation learning provides the backbone networks for many computer vision related tasks such as object detection, segmentation, image or video recognition, etc. [3]. Recent developments like NNCLR [4], SimSiam [5], Decoupled contrastive learning [2], CLIP [6], CAEs [7], are good examples of powerful feature extractors, and all employ some standard backbone network like ResNet [8] or EfficientNet [9]. Labeling the data is a costly operation, on the other hand, the main advantage of SSL models is their ability to learn better generic representations from the unlabelled data [10]. Foundational works like SimCLR [10] and SimSiam [5] have established that SSL models with slight finetuning (as low as 1% of the labeled data) can outperform their counterpart supervised models. Another advantage of SSL models is that they provide task-agnostic models which can easily be adapted using transfer learning to multiple kinds of downstream tasks (the tasks which are specialized cases of a larger generic task also known as the pretext task) [11].

Earlier models like the non-contrastive models (RotNet [11], Jigsaw [12]) used intelligently designed pretext tasks for providing the self-supervisory signal to the learning algorithm. These signals were based on some independent tasks like verifying the correct rotation [11], the correct sequence of frames [13], or the correct placement of tiles [12]. Recently, another branch of SSL methods, called contrastive learning (CL), has shown promising progress [10]. With better loss functions and image augmentations, these models have now exceeded the non-contrastive models. These contrastive learning based methods work by pushing closer the similar-looking (positive) samples and pushing apart non-similar class (negative) samples, without actually knowing the classes of these samples. However, recently, it was

shown that the positives generated using augmentations are not very semantically diverse [4]. To overcome this, it was suggested to use the nearest neighbors of the anchors (the samples whose positive is to be found), since this leads to better representations by learning from non-trivial positive samples [4]. However, in our experiments and analysis with NNCLR [4], we found that the quality of the support set plays a crucial role in learning better representations. At the beginning of training, the probability of finding a good nearest neighbor is low, and this can affect the overall learning in the SSL model. Based on these observations, this work presents stochastic pseudo nearest neighbors and the learning framework — pNNCLR.

The main objective of contrastive SSL methods is to employ a strategy or function, f , to arrange the latent space in such a way that similar class samples appear closer (attraction property) than distinct class samples (repulsion property) in the latent space. Nearest neighbor based methods try to amplify the diversity in the attraction process. The source of this diversity is the process of sampling the positives in the form of nearest neighbors and not augmented views. However, this amplification of diversity introduces a trade-off between the attraction and repulsion properties. Because, if the quality of the support set is low or the chosen nearest neighbors are incorrect (section 3.3), f may negatively impact the main objective by reducing the intended attraction and repulsion properties. To improve this trade-off, independent of the support set quality, we hypothesize modifying f such that the diversity in the attraction process is amplified favorably, i.e., the positive samples retain the semantic variations and, at the same time, are not unfavorably distinct from the anchor point. We accomplish this by reducing the magnitude of the resultant vector in the direction of the nearest neighbor by a factor. Although, this controls the diversification in the attraction process, however, it reduces the semantic quality. To avoid this, a stochastic prior is imposed during the sampling of positives. This allows the expansion of uncertainty to increase the semantic information. As a consequence of these adaptations, the positives become more semantically diverse and related to the anchor point, thereby, helping in learning better representations by the model. We also found that by employing a smooth-weight-updation approach, the effects of uncertainty, introduced by nearest neighbor based learning, can be stabilized to a significant extent.

We tested the proposed adaptations and found that they significantly improve the performance of the proposed method over our baseline, NNCLR [4], on image recognition tasks. Following this, we also tested it for the medical datasets and found a favorable performance. Following are the main contributions of this work:

- We studied the suitability of nearest neighbor based semantic information enrichment in CL, and introduced stochastic pseudo nearest neighbors (pNN) to control the quality of the positive samples in CL based SSL methods. To the best of our knowledge, we are first to introduce pNN approach.
- We showed that a smooth-weight-updation approach in NN based CL methods is highly useful in controlling the uncertainty in sampling. Using this, we propose our CL base method called pNNCLR, which significantly improves over our baseline NNCLR [4].
- We performed many experiments and ablation studies to empirically verify the superiority of our contribution through medical as well as non-medical datasets.

The remainder of the paper is organized as follows. Section 2 presents the related literature on representation learning methods. Section 3 presents the details of our baseline and the proposed method. Section 4 presents the implementation details, evaluation, and comparison of the results on different datasets. After this, the conclusion and appendix are presented.

2 Related Work

Representation learning methods have underpinned some of the recent highly successful pretrained networks and amazing feats of AI — GPT 3 [14], CLIP [6], SAM [15], ChatGPT [16], SEER [17]. These representation learning methods are mainly trained in a self-supervised manner. A couple of years earlier, self-supervised approaches were dominated by non-contrastive methods or by pretext task based methods (Context prediction [18], Jigsaw [12], RotNet [11]). However, the trend is shifting as the current best self-supervised methods are all based on some form of contrastive learning approach (SBCL [19], DINO [20]). Our baseline, NNCLR [4], is one such contrastive learning based method that employs nearest neighbor sampling. In this literature review, we cover the developments in SSL from the perspective of both — non-contrastive and contrastive — self-supervised methods. Table 1 provides a consolidated view of the literature.

2.1 Non-contrastive SSL methods

In the context of self-supervised learning, a *pretext task* refers to a puzzle or sub-task that is solved by the SSL model. The objective is to learn the underlying structure of the data by deriving a supervision signal from the sub-task in

Table 1: A consolidated literature review is presented for both — contrastive and non-contrastive SSL methods. Note that most of the backbones are CNN based.

Author	Year	Method	Contrastive	Backbone	Approach / Pretext-task
Doersch et al. [18]	2015	SpatialContext	✗	VGG	Predicting spatial context of a patch in relation to another patch in a spatially consistent array of nine patches.
Zhang et al. [21]	2016	CCEncoder	✗	In-house, VGG	Cross channel prediction using auto-encoder network.
Pathak et al. [22]	2016	ContextEncoder	✗	AlexNet	Inpainting of missing patch using context auto-encoders with channelwise fully-connected layers.
Misra et al. [13]	2016	ShuffleAndLearn	✗	SiameseAlexNet	Ordering of frames with sequence binary verification.
Noroozi et al. [12]	2016	ContextFreeNetwork	✗	SiameseAlexNet	Rearrangement of shuffled Jigsaw puzzle like sub-images.
Zhang et al. [23]	2017	SplitBrainAutoEncoder	✗	Channelwise AlexNet	Correct prediction of rearranged incomplete input channels.
Gidaris et al. [11]	2018	RotNet	✗	AlexNet	Correct prediction of rotated images.
Oord et al. [24]	2018	CPC	✓	ResNet-v2-101	Using contrastive predictive coding in PixelCNN auto-regressive recurrent neural networks for prediction of output embedding vectors.
Caron et al. [25]	2020	SwAV	✓	ResNet-50	Instead of pairwise contrastive loss, an online clustering of multiple views of same image is performed to learn the features and cluster assignments.
Chen et al. [26]	2020	iGPT-XL	✗	GPT-2 BERT	Auto-regressive prediction of pixels using transformers.
Chen et al. [10]	2020	SimCLR	✓	ResNet-50	A simple approach based on contrastive loss, non-linearity layer, augmentations and large batch sizes.
He et al. [27]	2020	MoCo	✓	ResNet-50	An online dictionary approach for contrastive learning using memory bank and momentum contrast.
Grill et al. [28]	2020	BYOL	✓	ResNet-50	Does not use negative pairs for contrastive loss while using momentum contrast.
Chen et al. [5]	2021	SimSiam	✓	ResNet-50	Uses a simple Siamese network without negative pairs, large batch size, momentum contrast.
Caron et al. [20]	2021	DINO	✓	ViT-S/16	Contrastive learning on vision transformers using a codistillation approach.
Goyal et al. [17]	2021	SEER	✓	RegNet-Y	SwAV method is used to train large SSL model on very large dataset in the wild.
Dwibedi et al. [4]	2021	NNCLR	✓	ResNet-50	Uses a nearest neighbor approach to increase the semantic variation during learning.
Xie et al. [29]	2022	SimMIM	✗	ViT-B	Correct prediction of patch level masked images using transformers.
Yeh et al. [2]	2022	Decoupled CLR	✓	ResNet-50	Remove the positive term from the denominator of the InfoNCE loss to reduce the positive-negative-coupling.
Zhang et al. [30]	2023	ADCLR	✓	ViT-S/16	Transformer based approach for dense contrastive learning by balancing global and patch-level losses.
Hou et al. [19]	2023	SBCL	✓	ResNet-50	A hierarchical online clustering like SwAV to balance the emphasis between head class and long-tailed class.

an unsupervised manner, i.e., without relying on any labeled data [18]. Doersch et al. explored spatial context as a supervision signal for training visual representations [18]. Their approach involved dividing a region in image into 9 patches, then sampling pairs from these patches and training the model to predict the relative position of a patch given another patch from the pair. They achieved unsupervised object discovery and improved performance on object detection tasks. Zhang et al. used cross channel color space prediction as a pretext task [21, 23]. They used a CNN to predict ab color space from L channel of the CIE Lab^* color space. It was found that colorization could be a useful option for learning representations for vision tasks. Pathak et al. also used context information for their inpainting pretext task by forcing their context encoding CNN to predict the missing region in an input image [22]. Although predicting the entire region is an under constrained task, however, their approach produced strong image representations. Another line of work (Shuffle learn [13], Sequence sorting [31], Sustained order verification [32, 33], Odd one out [34]), used frame order prediction as the pretext task. These models learned meaningful image representations for vision tasks. However, it was not as strong as the representations learned by other pretext tasks, like context prediction or spatial rearrangement. Noroozi et al. proposed an even more challenging pretext task of sorting all nine pieces of

a Jigsaw puzzle [12]. They also suggested several shortcut prevention approaches as they emphasized — “A good self-supervised task is neither simple nor ambiguous.” Gidaris et al. proposed a simple rotation prediction as the pretext task for CNNs [11]. The objective was to predict the angle of rotation from 0, 90, 180, 270 degrees. Rotation turned out to be a simple yet powerful SSL strategy since it does not leave any easily detectable low-level visual shortcut for trivial feature learning. Chen et al. adapted a GPT-2 scale transformer model from Masked Language Modeling (MLM) to Masked Image Modeling (MIM) on pixels of down-scaled images [26]. Objective of the pretext task was to auto-regressively predict the masked pixels in the transformer output in a BERT-like sense. Following the same line, Zhou et al. introduced an online visual tokenizer for MIM [35]. They showed that better semantics could be learned by simultaneously training the tokenizer with the MIM transformer through knowledge distillation. Xie et al. simplified the previous transformer based masked prediction pretext task methods by dropping blockwise masking and tokenization [29]. Their model achieved competitive results with just linear probing.

2.2 Contrastive SSL methods

Although, pretext based methods achieved good representations, however, Misra et al. showed that they all followed a covariant style of modeling [36]. Misra et al. advocated the superiority of an invariant style of modeling over a covariant. Their work sits between non-contrastive and contrastive SSL methods. The main contribution is the noise contrastive estimation formulation which involves the generation of positive and negative pairs using the Jigsaw objective [12]. Contrastive SSL methods differ in their approach by including the pretext task in the model architecture itself in the form of augmentations. Additionally, the model objective changes from equivariance (where the model tries to adjust itself according to the variation in input) to invariance (where the model ignores the changes in the input in order to become agnostic to those transformations). To be specific, the SSL supervision signal is derived by enforcing the equivalence of multiple views of the same input image [10]. One such initial work by Oord et al. proposed Contrastive Predictive Coding (CPC) for unsupervised representation learning [24]. They applied noise contrastive loss (NCL) over future predictions in latent space of auto-regressive models for speech, text, and images. An important aspect of their NCL formulation was inclusion of negative samples. Later it was picked up and improved by Chen et al. [10]. They proposed a simple contrastive learning approach in which they emphasized on compositions in data augmentation, role of non-linear transformations in top layers, and larger batch size. He et al. proposed the idea of dictionary look-up by maintaining a dictionary of encoded keys as negatives for contrastive learning [27]. This allowed keeping a larger set than the batch size as negatives. Similar to He et al., Girll et al. proposed online and target network based contrastive learning where the target network avoids direct gradient flow and takes updates from the online network [28]. They also showed that the setup does not require negative samples for training the network. To reduce the overall computation in contrastive SSL methods, Caron et al. proposed to avoid pairwise comparisons by employing online clustering of the representations and by enforcing consistency in cluster assignments of representations corresponding to different views of the same sample [25]. Chen et al. refined the contrastive SSL aspects of previous works [5]. They trained a Siamese network with contrastive loss but without negative sample pairs and without large batch sizes. They avoided trivial solutions and attained competitive performance by avoiding gradient propagation in one of the branches of the Siamese network. Caron et al. proposed a self-supervised knowledge distillation approach called DINO [20]. They showed that vision transformers learn better semantic segmentation and k -NN features than CNNs. Goyal et al. validated the contemporary contrastive SSL approaches in the wild by training with one billion random images [17]. Yeh et al. proposed decoupling the positive samples from the denominator of the InfoNCE contrastive loss to remove the negative-positive-coupling effect in contrastive SSL methods [2]. Zhang et al. introduced query patches for contrasting in addition to global contrasting [30]. Nearest neighbor based methods like [4, 19] emphasized increasing semantic variation by sampling the nearest neighbors in the latent space. The proposed work is similar in spirit to the nearest neighbor sampling based works.

3 Method

In this section, we first formalize the representation learning problem. After this, the NNCLR approach is described, and finally, we present the details of the proposed method.

3.1 Problem

Representation learning aims to learn a model which can map its inputs to corresponding vectors in such a way that for any two closely related inputs, their vectorial representations are also close, and far away for any two unrelated or distinctly related inputs. For a given dataset \mathcal{X} having images $x_i | i \in [1, N]$, we wish to learn a homomorphism, model \mathcal{M}_θ parameterized by θ , such that for any three inputs x_i, x_j and x_k , \mathcal{M}_θ gives three corresponding vectors $\mathbf{u}_i, \mathbf{u}_j$, and \mathbf{u}_k respectively, such that the following condition holds:

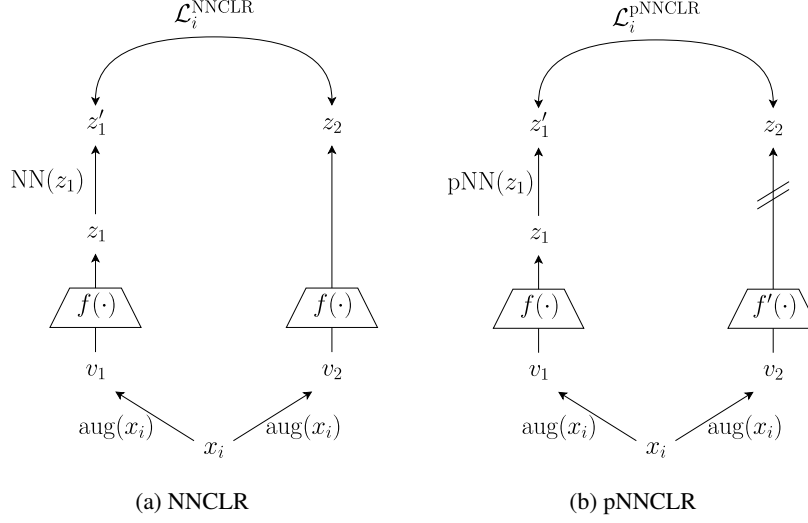


Figure 1: Model diagrams of NNCLR and pNNCLR methods. The cross sign in pNNCLR denotes stop-gradient operation. $f(\cdot)$ is the backbone encoder network. $\text{aug}(x_i)$ is a random transformation function that generates a new view for x_i . $\text{pNN}(\cdot)$ is the proposed pseudo nearest neighbor sampling function.

$$d_x(x_i, x_j) \star d_x(x_i, x_k) \Leftrightarrow d_v(\mathbf{u}_i, \mathbf{u}_j) \star d_v(\mathbf{u}_i, \mathbf{u}_k), \quad (1)$$

where, d_x and d_v represent the distance function in image and vector spaces respectively, and \star is any relational operator like \ll .

3.2 NNCLR

Contrastive learning methods like SimCLR [10] or BYOL [28] train by generating two augmented views v_1, v_2 for the same input x_i . During the loss calculation, embeddings corresponding to v_1, v_2 are treated as positives, whereas embeddings corresponding to all other $x_j | j \neq i$ are treated as negatives to v_1, v_2 . A variant of InforNCE loss [24] like

$$\mathcal{L}_i^{\text{SimCLR}} = -\log \frac{\exp(z_i \cdot z_i^+ / \tau)}{\sum_{k=1}^n \exp(z_i \cdot z_k^+ / \tau)}, \quad (2)$$

is used, where z_i is the embedding or the vector corresponding to the view v_1 , z_i^+ is the positive pair of z_i . The set, $z_k^+ | k \in [1, n]$, denotes all embeddings in the mini-batch (with size n), including the positive z_i^+ and negatives $z_k^- | k \neq i$. τ denotes the softmax temperature. The operation, $\mathbf{u} \cdot \mathbf{v}$ in Eq. (2), represents a similarity function, generally a dot product of the normalized vectors \mathbf{u}, \mathbf{v} or their cosine similarity. NNCLR improves this approach by replacing z_i with its nearest neighbor, $\text{NN}(z_i)$, as shown in Fig. 1a. The nearest neighbor is found from a support set Q , which is maintained by inserting the current batch items and removing the oldest batch items from it in a first-in-first-out manner for every training iteration. Using $\text{NN}(z_i)$, NNCLR loss function for $x_i \in \text{batch}\{x_k | 1 \leq k \leq n\}$ becomes:

$$\mathcal{L}_i^{\text{NNCLR}} = -\log \frac{\exp(\text{NN}(z_i) \cdot z_i^+ / \tau)}{\sum_{k=1}^n \exp(\text{NN}(z_i) \cdot z_k^+ / \tau)}. \quad (3)$$

3.3 pNNCLR

Although the intuition of semantic variability behind NNCLR has shown promising results compared to other recent developments in contrastive learning methods [4], however, NNCLR achieves this at a cost, since the probability of finding a hard nearest neighbor, from the support set Q , belonging to the same class is quite low ($\sim 50\%$) at the beginning of training (details in A). I.e., if $\text{class}(\cdot)$ denotes the class membership function, the approximate (since it

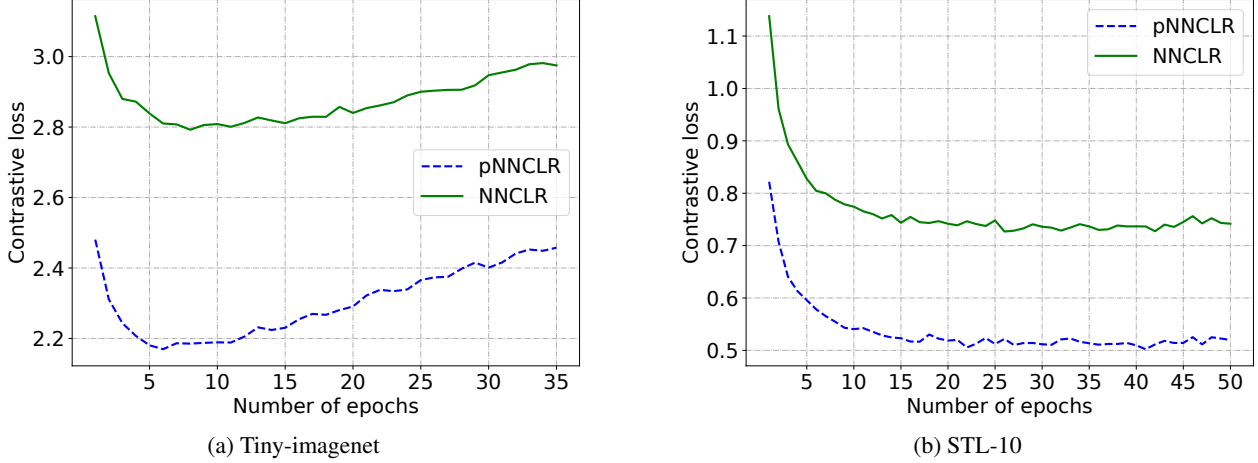


Figure 2: Loss plots of NNCLR and pNNCLR methods on Tiny-imagenet and STL-10 datasets. Note, NNCLR incurs a higher loss right from the beginning of training.

depends on the support set size) maximal probability, $P[\text{class}(\text{NN}(z_i)) = \text{class}(z_i)]$, that the nearest neighbor belongs to the same class as z_i or x_i is around 50% (details in A), which means there is a 50% chance that the nearest neighbor is from a different class. This reduces the inter-class variation of the representations, leading to a decline in performance. This was also seen in the NNCLR method’s loss plots (Fig. 2). NNCLR incurs a higher loss in the beginning of training.

If we carefully investigate the intuition behind NNCLR, we will find that it is trying to increase the semantic variability between the two views v_1, v_2 . However, by doing so, it is also dispersing the intra-class representations to have a larger mean deviation. These two ideas are inversely related. To overcome this trade-off, this work proposes to use soft or pseudo nearest neighbor function, $\text{pNN}(\cdot)$, in place of $\text{NN}(\cdot)$, to perform better irrespective of the probability $P[\text{class}(\text{NN}(z_i)) = \text{class}(z_i)]$. The proposed method is called, pNNCLR, pseudo/probabilistic nearest neighbor CLR (Fig. 1b). Function $\text{pNN}(\cdot)$, works by sampling a point z_i'' in the direction of the vector $z_i \overrightarrow{\text{NN}(z_i)}$ such that the resultant vector $z_i \overrightarrow{z_i''}$ has a shorter magnitude than $z_i \overrightarrow{\text{NN}(z_i)}$. This shortness is controlled by a scalar hyperparameter $\alpha \in (0, 1)$ as:

$$z_i'' \leftarrow z_i + (1 - \alpha)(\text{pNN}(z_i) - z_i). \quad (4)$$

While the probability $P[\text{class}(\text{NN}(z_i)) = \text{class}(z_i)]$ improves by using z_i'' over z_i , some semantic variability is lost. To dilute this effect, we found that we can stochastically resample in the vicinity of z_i'' . This is done by using a Gaussian prior with mean z_i'' and standard deviation which is a fraction, β , of $\|z_i \overrightarrow{z_i''}\|$, where $\|\cdot\|$ denotes magnitude of a vector. This is shown in Eq. (5).

$$z_i' \sim \mathcal{N}(z_i'', \beta \|z_i \overrightarrow{z_i''}\|), \quad (5)$$

where, \mathcal{N} stands for a normal distribution, and $\beta \in (0, 1)$ is a scalar constant. Due to higher uncertainty in NN based approach, we slow down the weight updation process of the encoder network $f'(\cdot)$, shown in Fig. 1b, by stopping the gradient flow in non $\text{pNN}(\cdot)$ branch (also called the target branch [28]). Providing a smoother updation of weights by using following:

$$\theta_{f'} \leftarrow \lambda \theta_{f'} + (1 - \lambda) \theta_f, \quad (6)$$

where, θ stands for network parameters, f is the online network, f' is the target network, $\lambda \in (0, 1)$ is a constant that controls the effect of f over f' . By replacing the nearest neighbor function in Eq. 3, we obtain the loss for pNNCLR, as:

$$\mathcal{L}_i^{\text{pNNCLR}} = -\log \frac{\exp(\text{pNN}(z_i) \cdot z_i^+ / \tau)}{\sum_{k=1}^n \exp(\text{pNN}(z_i) \cdot z_k^+ / \tau)}, \quad (7)$$

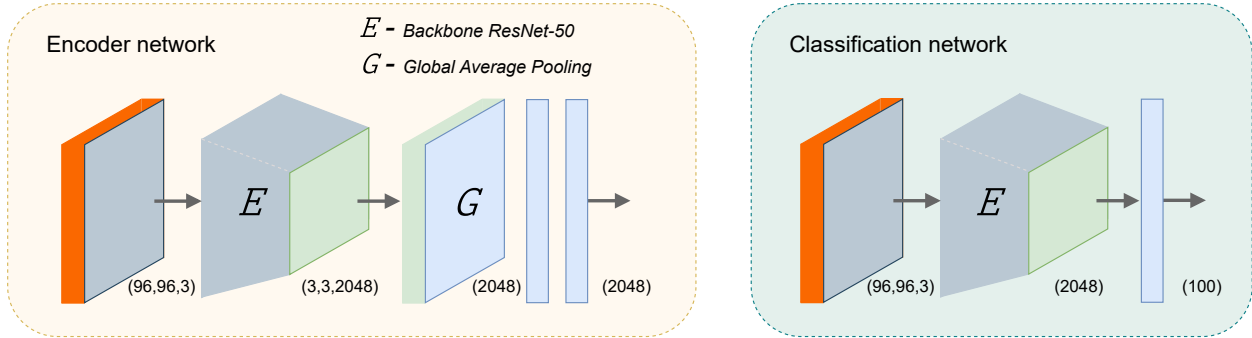


Figure 3: Proposed pNNCLR architecture details considering Cifar-100 as the downstream task. Left, architecture for contrastive SSL training. Right, linear probing adaptation on Cifar-100 dataset.

using this, the loss for the entire mini-batch, b , of size N_b becomes:

$$\mathcal{L}_b^{pNNCLR} = \frac{1}{N_b} \sum_{i=1}^{N_b} \mathcal{L}_i^{pNNCLR}. \quad (8)$$

The total loss, \mathcal{L}^{pNNCLR} , is a symmetrized loss obtained by swapping the views v_1, v_2 in Eq. (8), as:

$$\mathcal{L}^{pNNCLR} = \mathcal{L}_b^{pNNCLR}(v_1, v_2) + \mathcal{L}_b^{pNNCLR}(v_2, v_1). \quad (9)$$

4 Experiments

This section first describes the experimental arrangement. Next, the implementation and dataset related details are presented. After this, the results of the proposed pNNCLR approach are compared with the recent methods for SSL for the linear evaluation task. Towards the end, some ablations, discussion on results, and future directions are presented.

4.1 Implementation details

We have used the batch size of 64, and 10000 as the size of the support set. The embedding size was kept at 2048. The optimizer was Adam, and the learning rate was set to 0.001. The images for every dataset were resized to 96×96 . ResNet-50 [8] was used as the base encoder network. The final prediction layer of ResNet was removed, and a Global average pooling was used for flattening, followed by two dense layers having 2048 nodes, and a batch norm was present between these two dense layers as shown in Fig. 3, encoder network. During testing, the encoder was frozen after the fine-tuning, and an additional dense layer having the softmax activation was used for classification (linear probing), as shown in Fig. 3, classification network. Five non-medical datasets (STL-10, Cifar-10,100, Tiny-imagenet, Pascal-VOC) and three medical datasets (Blood-MNIST, PCAM, Path-MNIST) were used for evaluation and comparison purposes. Details of these datasets and their splitting strategy for training and testing purposes is provided in the next section. Top-1 accuracy was the metric used for all our experiments unless stated otherwise.

4.2 Datasets

STL-10 It is a standard dataset derived from Imagenet [37] for developing self-supervised learning algorithms. It has 100000 unlabeled and 13000 labeled images from 10 classes (like bird, cat, truck) [38]. All models reported here, were trained for 100 epochs on this dataset.

Cifar-10 and Cifar-100 Each of these datasets consists of 60000 images [39]. Cifar-10 consists of 10 classes, whereas Cifar-100 consists of 100 classes. General class labels are bird, dog, ship, horse, truck, etc.

Tiny-imagenet This dataset contains 120000 images from 200 classes [40].

Pascal-VOC This dataset contains 20 classes like vehicles, airplanes, animals, etc. It contains approximately 3000 images.

Table 2: Results are shown for Top-1 accuracy on the non-medical datasets on the image recognition task. For each dataset, **best** method is marked in bold, second best is underlined.

Method	STL-10	Cifar-10	Cifar-100	Tiny-imagenet	Pascal-VOC	Mean (Top-1 acc.)
Baseline (NNCLR [4])	0.7548	0.9441	0.7763	0.3929	-	0.7170
MoCo v2 [27]	<u>0.8355</u>	0.9411	0.7804	0.4651	<u>0.4900</u>	<u>0.7555</u>
BYOL [28]	0.8044	0.9456	<u>0.7882</u>	0.4577	-	0.7489
SimCLR [10]	0.7974	0.9428	0.7812	<u>0.4660</u>	-	0.7468
SimSiam [5]	0.8067	0.9418	0.7811	0.3284	-	0.7145
DINO [20]	0.8200	0.9459	0.7809	0.3161	-	0.7157
Decoupled CLR [2]	0.8343	<u>0.9498</u>	0.7812	0.4245	-	0.7474
Proposed method (pNNCLR)	0.8413	0.9582	0.7885	0.4856	0.5066	0.7684

Table 3: Results are shown for Top-1 accuracy on the medical datasets on the image recognition task. For each dataset, **best** method is marked in bold, second best is underlined.

Method	Blood-MNIST	PCAM	Path-MNIST	Mean (Top-1 acc.)
Baseline (NNCLR [4])	0.7969	0.8849	0.8292	0.8370
MoCo v2 [27]	0.8906	0.9180	0.8562	0.8882
BYOL [28]	0.8516	0.8868	0.8365	0.8583
SimCLR [10]	0.8594	0.8951	0.8552	0.8699
SimSiam [5]	0.8594	0.8397	0.7917	0.8302
DINO [20]	0.7500	0.7824	0.7698	0.7674
Decoupled CLR [2]	0.8281	0.8884	<u>0.8615</u>	0.8593
Proposed method (pNNCLR)	<u>0.8672</u>	<u>0.9025</u>	0.8708	<u>0.8801</u>

Blood-MNIST and Path-MNIST Both of these datasets belong to a large collection of biomedical images [41]. Blood-MNIST has approximately 17000 images belonging to 8 classes from blood cell microscopy. Path-MNIST has 9 classes having approximately 100000 images of Colon pathology.

PCAM or PatchCamelyon It is a binary image classification dataset [42] having approximately 327000 images extracted from histopathologic scans of lymph node sections to indicate the presence of metastatic tissue.

Features learned from STL-10 were used to apply transfer learning to other datasets. Approximately $\sim 2\%$ of the images were used for applying transfer learning using a linear layer on the pretrained encoder model.

4.3 Results

To evaluate the performance of the proposed method, it is compared with very competitive recent benchmark self-supervised learning works. The results are presented in Table 2 and 3 for non-medical and medical types of datasets, respectively. Our baseline work is the NNCLR method [4], which was published in ICCV 2021. MoCo [27] and BYOL [28] are momentum contrast based approaches for contrastive learning, and appeared in CVPR 2020 and NeurIPS 2020 respectively. SimCLR [10] is the baseline approach of NNCLR, and was published in PMLR 2020. SimSiam [5] showed that even without using the negative samples, good performance could be achieved in SSL. It was published in CVPR 2021. DINO [20] is a vision transformer based method and was published in ICCV 2021. Decoupled CLR [2] removed the positives from the denominator of the InfoNCE loss [24] and proposed a simple CL method which was published in ECCV 2022.

Table 2 presents the results for non-medical datasets. The proposed method, pNNCLR, achieved the highest Top-1 accuracy for each of the datasets among all methods. It surpassed the baseline, NNCLR, by a maximum $\sim 8\%$ on STL-10 and Tiny-imagenet, and by $\sim 4\%$ on average over all datasets. The second best performance was attained by MoCo [27], which is $\sim 1\%$ less than pNNCLR, on average. Table 3 presents the results for medical datasets. For the Blood-MNIST dataset, MoCo attained the best results with an accuracy of 89.06% while the proposed pNNCLR method lagged behind by $\sim 2\%$; however, it performed $\sim 7\%$ better than the baseline NNCLR. On the PCAM dataset, again the best performance was attained by MoCo while pNNCLR lagged behind by $\sim 1\%$. On the Path-MNIST dataset, pNNCLR attained the best results while the second best performance was attained Decoupled CLR method. On average, pNNCLR lagged behind by the best performance by less than 1% while surpassing the baseline NNCLR

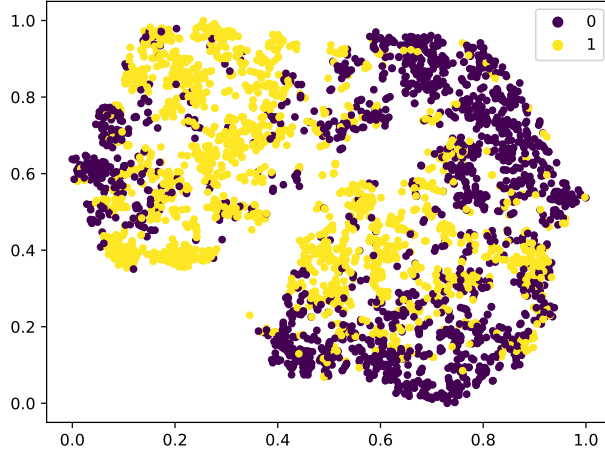


Figure 4: T-sne plot of the representations learned by the proposed pNNCLR method on the PatchCamelyon (PCAM) medical dataset.

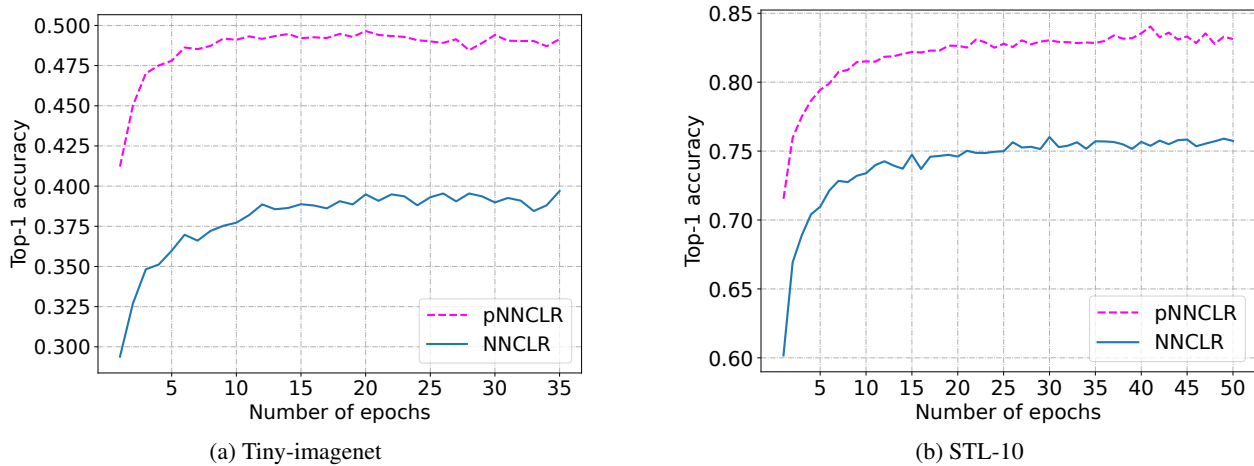


Figure 5: Top-1 accuracy plots of the baseline NNCLR and proposed pNNCLR methods on Tiny-imagenet and STL-10 datasets.

by $\sim 4\%$. Figure 4 presents a low dimensional view of the representations learned by the proposed pNNCLR method on the PCAM dataset for the binary classification of the presence of metastatic tissues in lymph node scans. Figure 5 shows the accuracy plots of the proposed pNNCLR method vs. the baseline NNCLR, on the Tiny-imagenet and STL-10 datasets. It can be noted that pNNCLR attains comparatively better performance right from the beginning phase of training. The cause for this behavior is also explained in the section 3.3. While, for both methods, the performance saturates asymptotically, showing a similar trend.

These results indicate that the proposed pNNCLR method performs notably better than the baseline NNCLR method. pNNCLR performs better than other SSL methods on non-medical datasets and comparatively on medical datasets. MoCo performed comparably well with respect to the proposed method.

4.4 Ablations

The ablation study was performed with the baseline NNCLR and proposed method on the STL-10 dataset. In the first ablation, we examined the effect of each proposed modification to the baseline NNCLR method. Table 4 reports the corresponding results. In that, *swu* denotes smooth weight updation, and *pNN* denotes pseudo nearest neighbor sampling. In Table 4, modifying NNCLR with *swu*, pushes the accuracy by $\sim 7\%$. Modifying NNCLR with (*swu+pNN*), pushes the accuracy further by $\sim 1\%$. Modifying NNCLR with (*swu+pNN+noise*) further pushes the accuracy to 84.13%. These results show that *swu* significantly stabilizes the uncertainty in the learning process. Table 5 presents variation in

Table 4: Effect of modifications in the baseline NNCLR method with smooth-weight-update denoted as (swu), pseudo neighborhood as (pNN), and addition of noise in sampling. Top-1 accuracy is reported for each experiment on the STL-10 dataset.

Method	Top-1 accuracy (\uparrow)
Baseline (NNCLR [4])	0.7548
pNNCLR (swu)	0.8257
pNNCLR (swu + pNN)	0.8386
pNNCLR (swu + pNN + noise)	0.8413

Table 5: Ablation on the hyperparameters (β and α) of the proposed pNN(\cdot) (pseudo nearest neighbor) sampling approach. Top-1 accuracy is reported on the STL-10 dataset.

Variation in hyperparameters	
β	Top-1 accuracy
0.05	0.8376
0.10	0.8413
α	
0.05	0.8286
0.10	0.8295
0.15	0.8321
0.25	0.8386

the hyperparameters α — the pseudo sampling control hyperparameter, and β — the noise control hyperparameter. A value of 0.10 provided a better result over $\alpha = 0.05$. Similarly, $\beta = 0.25$ provided the best results. Table 6, 7, 8, provide results of the ablation study on the embedding size, support-set size and batch size. Table 6 shows that the performance of the proposed method increases as the embedding vector size increases. On the other hand, the baseline method’s performance maxes out at 2048. For this reason, we used 2048 as the embedding size in all our experiments for all SSL methods. Table 7 shows that the performance of the proposed method maxes out at a queue size of 10000. Performance of the baseline method maxes out at 20000; however, it is comparable to its performance at 10000. Therefore, we took 10000 as the size of the support set in all our experiments for all SSL methods. Table 8 shows that the proposed and the baseline methods achieve their best performance at a batch size of 64. Therefore, 64 was used as the batch size in all our experiments for all SSL methods.

4.5 Future directions

In our experiments, we noticed that the size of the support set affects the performance of the SSL method. This has also been observed by other researchers. Conversely, it entails that we need to explore the role of nearest neighbors or pseudo nearest neighbors in other types of SSL methods. We hypothesize that the performance of other SSL methods may benefit from increased diversification of the semantic information. We can also move in the direction of improving the quality of nearest neighbors or the support set as it directly affects the learning in the SSL model. We can also experiment with how effective the features learned by different SSL methods are on the medical image segmentation task. We can also explore the effect of model agnostic variance regularization functions in NNCLR or pNNCLR [43].

5 Conclusion

In this paper, we studied the problem of contrastive self-supervised learning. We covered the development of the field from non-contrastive methods to contrastive methods. It was found that the nearest neighbor sampling based methods were good at increasing semantic variations during unsupervised SSL learning. However, the shortcomings of these methods were also discussed. Further, we proposed pNNCLR, a pseudo nearest neighbor based contrastive learning method, to overcome the weakness of the widely used NNCLR method. We showed how the choice of nearest neighbors in the support set can affect the quality of the learned representations. To avoid this, pNNCLR introduced the use of

Table 6: Effect of using different embedding sizes on the baseline and the proposed method. Top-1 accuracy is reported on the STL-10 dataset.

Embedding size	NNCLR [4]	Proposed method
512	0.6061	0.7986
1024	0.6580	0.8143
2048	0.7548	0.8413
4096	0.7537	0.8429

Table 7: Effect of using different support-set or queue sizes. Top-1 accuracy is reported for the baseline and the proposed method on STL-10 dataset.

Queue size	NNCLR [4]	Proposed method
5000	0.7191	0.8329
10000	0.7548	0.8413
15000	0.7540	0.8407
20000	0.7555	0.8411

Table 8: Effect of using different batch sizes. Top-1 accuracy is reported for the baseline and the proposed method on the STL-10 dataset.

Batch size	NNCLR [4]	Proposed method
16	0.7051	0.7916
32	0.7141	0.8178
64	0.7548	0.8413

pseudo nearest neighbors (pNN) with stochastic sampling. Further, a smooth weight updation strategy was also used to stabilize the uncertainty in the learning process. The proposed modifications and multiple recent SSL methods were evaluated on different medical and non-medical standard datasets. Various ablations were performed to fine-tune the hyperparameters. The experiments show that the proposed sampling strategy performs significantly better than the baseline NNCLR approach while competing favorably against the other recent SSL methods.

A Same class nearest neighbor probability calculation

Suppose, the dataset \mathcal{D} on which we are training our SSL network contains classes c_1, c_2, \dots, c_{N_c} , where N_c is the number of classes. Each class c_i has N_e number of items, i.e., we assume that we have a balanced dataset. When choosing a nearest neighbor $\text{NN}(x_i)$ or $\text{NN}(z_i)$ for a view of the input x_i , from randomly formed support set Q with cardinality N_q , the approximate maximal probability, $P[\psi]$ or $P[\text{class}(\text{NN}(z_i)) = \text{class}(z_i)]$, can be calculated as follows. Here, z_i is the corresponding embedding of one of the views of x_i . We assume that every individual item $x \in \mathcal{D}$ has an equal probability of being randomly selected for forming the support set Q . Then, $P[\psi]$ can be defined as:

$$\begin{aligned}
 P[\psi] &= P[A \cap B] = P[A|B] \cdot P[B] \\
 \text{where, } A &: \text{class}(\text{NN}(z_i)) = \text{class}(z_i), \text{ if } P[B] = 1 \\
 B &: |\{q_i | q_i \in Q \text{ and } \text{class}(q_i) = \text{class}(z_i)\}| \geq 1,
 \end{aligned}
 \tag{10}$$

where $|\cdot|$ denotes the set cardinality. In other words, $P[\psi]$ is the probability of the nearest neighbor function $\text{NN}(\cdot)$ choosing the correct class. If $\binom{\cdot}{\cdot}$ denotes the binomial coefficient, the probability of the support set Q getting at least one item from the correct class, $P[B]$, when items in Q are randomly picked from \mathcal{D} with an equal probability, becomes:

$$P[B] = 1 - P[\bar{B}].
 \tag{11}$$

$$P[\bar{B}] = \frac{\binom{(N_c - 1)N_e}{N_q}}{\binom{N_c N_e}{N_q}}. \quad (12)$$

using (12) in (11), we get

$$\begin{aligned} P[B] &= 1 - \frac{\binom{(N_c - 1)N_e}{N_q}}{\binom{N_c N_e}{N_q}} \\ &= 1 - \frac{(N_c N_e - N_e)!(N_c N_e - N_q)!}{(N_c N_e - N_e - N_q)!(N_c N_e)!} \\ &= 1 - \frac{N_c N_e - N_q}{N_c N_e} \cdot \frac{N_c N_e - 1 - N_q}{N_c N_e - 1} \dots \frac{N_c N_e - N_e + 1 - N_q}{N_c N_e - N_e + 1}. \end{aligned} \quad (13)$$

$$\frac{N_c N_e - N_q}{N_c N_e} \cdot \frac{N_c N_e - 1 - N_q}{N_c N_e - 1} \dots \frac{N_c N_e - N_e + 1 - N_q}{N_c N_e - N_e + 1} < \left(\frac{N_c N_e - N_q}{N_c N_e} \right)^{N_e}. \quad (14)$$

$$\frac{N_c N_e - N_q}{N_c N_e} \cdot \frac{N_c N_e - 1 - N_q}{N_c N_e - 1} \dots \frac{N_c N_e - N_e + 1 - N_q}{N_c N_e - N_e + 1} > \left(\frac{N_c N_e - N_e + 1 - N_q}{N_c N_e - N_e + 1} \right)^{N_e}. \quad (15)$$

Using Eq. (13), Eq. (14) and Eq. (15), we get a lower and upper bound on $P[B]$ as:

$$1 - \left(\frac{N_c N_e - N_q}{N_c N_e} \right)^{N_e} < P[B] < 1 - \left(\frac{N_c N_e - N_e + 1 - N_q}{N_c N_e - N_e + 1} \right)^{N_e}. \quad (16)$$

Now, let us consider two scenarios, both with a fixed value of $N_q = 10000$. First, when we have a very large dataset where $N_c = 1000$ and $N_e = 1000$, we get $P[B] \simeq 0.9999$, using Eq. (16). Second, when we have a relatively smaller dataset where $N_c = 100$ and $N_e = 100$, or $N_c = 10$ and $N_e = 1000$, we get $P[B] \simeq 1$, using Eq. (16). Hence, the probability $P[B]$ stays $\simeq 1$ for both smaller as well as larger size datasets. This changes Eq. (10) as:

$$P[\psi] = P[\text{class}(\text{NN}(z_i)) = \text{class}(z_i)] = P[A], \quad (17)$$

which implies that the maximal probability, $P[\psi]$, is proportionate to the probability of choosing the correct class, which in turn depends on the quality of the representations learned by the model \mathcal{M}_θ . As we know that \mathcal{M}_θ is randomly initialized and stays quite random for the starting epochs, the probability of choosing the correct class becomes $P[\psi] \simeq 0.5$, which is as good as a random selection.

References

- [1] Nikolas Adaloglou, Felix Michels, Hamza Kalisch, and Markus Kollmann. Exploring the limits of deep image clustering using pretrained models. *arXiv preprint arXiv:2303.17896*, 2023. [1](#)
- [2] Chun-Hsiao Yeh, Cheng-Yao Hong, Yen-Chi Hsu, Tyng-Luh Liu, Yubei Chen, and Yann LeCun. Decoupled contrastive learning. In *European Conference on Computer Vision*, pages 668–684. Springer, 2022. [1](#), [3](#), [4](#), [8](#)

- [3] Yuchao Zheng, Chen Li, Xiaomin Zhou, Haoyuan Chen, Hao Xu, Yixin Li, Haiqing Zhang, Xiaoyan Li, Hongzan Sun, Xinyu Huang, et al. Application of transfer learning and ensemble learning in image-level classification for breast histopathology. *Intelligent Medicine*, 3(02):115–128, 2023. 1
- [4] Debidatta Dwibedi, Yusuf Aytar, Jonathan Tompson, Pierre Sermanet, and Andrew Zisserman. With a little help from my friends: Nearest-neighbor contrastive learning of visual representations. In *Proceedings of the IEEE/CVF International Conference on Computer Vision*, pages 9588–9597, 2021. 1, 2, 3, 4, 5, 8, 10, 11
- [5] Xinlei Chen and Kaiming He. Exploring simple siamese representation learning. In *Proceedings of the IEEE/CVF conference on computer vision and pattern recognition*, pages 15750–15758, 2021. 1, 3, 4, 8
- [6] Alec Radford, Jong Wook Kim, Chris Hallacy, Aditya Ramesh, Gabriel Goh, Sandhini Agarwal, Girish Sastry, Amanda Askell, Pamela Mishkin, Jack Clark, et al. Learning transferable visual models from natural language supervision. In *International conference on machine learning*, pages 8748–8763. PMLR, 2021. 1, 2
- [7] Xiaokang Chen, Mingyu Ding, Xiaodi Wang, Ying Xin, Shentong Mo, Yunhao Wang, Shumin Han, Ping Luo, Gang Zeng, and Jingdong Wang. Context autoencoder for self-supervised representation learning. *arXiv preprint arXiv:2202.03026*, 2022. 1
- [8] Kaiming He, Xiangyu Zhang, Shaoqing Ren, and Jian Sun. Deep residual learning for image recognition. In *Proceedings of the IEEE conference on computer vision and pattern recognition*, pages 770–778, 2016. 1, 7
- [9] Brett Koonce and Brett Koonce. Efficientnet. *Convolutional Neural Networks with Swift for Tensorflow: Image Recognition and Dataset Categorization*, pages 109–123, 2021. 1
- [10] Ting Chen, Simon Kornblith, Mohammad Norouzi, and Geoffrey Hinton. A simple framework for contrastive learning of visual representations. In *International conference on machine learning*, pages 1597–1607. PMLR, 2020. 1, 3, 4, 5, 8
- [11] Spyros Gidaris, Praveer Singh, and Nikos Komodakis. Unsupervised representation learning by predicting image rotations. *arXiv preprint arXiv:1803.07728*, 2018. 1, 2, 3, 4
- [12] Mehdi Noroozi and Paolo Favaro. Unsupervised learning of visual representations by solving jigsaw puzzles. In *European conference on computer vision*, pages 69–84. Springer, 2016. 1, 2, 3, 4
- [13] Ishan Misra, C Lawrence Zitnick, and Martial Hebert. Shuffle and learn: unsupervised learning using temporal order verification. In *Computer Vision–ECCV 2016: 14th European Conference, Amsterdam, The Netherlands, October 11–14, 2016, Proceedings, Part I 14*, pages 527–544. Springer, 2016. 1, 3
- [14] Tom Brown, Benjamin Mann, Nick Ryder, Melanie Subbiah, Jared D Kaplan, Prafulla Dhariwal, Arvind Nee-lakantan, Pranav Shyam, Girish Sastry, Amanda Askell, et al. Language models are few-shot learners. *Advances in neural information processing systems*, 33:1877–1901, 2020. 2
- [15] Alexander Kirillov, Eric Mintun, Nikhila Ravi, Hanzi Mao, Chloe Rolland, Laura Gustafson, Tete Xiao, Spencer Whitehead, Alexander C Berg, Wan-Yen Lo, et al. Segment anything. *arXiv preprint arXiv:2304.02643*, 2023. 2
- [16] Yiheng Liu, Tianle Han, Siyuan Ma, Jiayue Zhang, Yuanyuan Yang, Jiaming Tian, Hao He, Antong Li, Mengshen He, Zhengliang Liu, et al. Summary of chatgpt/gpt-4 research and perspective towards the future of large language models. *arXiv preprint arXiv:2304.01852*, 2023. 2
- [17] Priya Goyal, Mathilde Caron, Benjamin Lefau-deux, Min Xu, Pengchao Wang, Vivek Pai, Mannat Singh, Vitaliy Liptchinsky, Ishan Misra, Armand Joulin, et al. Self-supervised pretraining of visual features in the wild. *arXiv preprint arXiv:2103.01988*, 2021. 2, 3, 4
- [18] Carl Doersch, Abhinav Gupta, and Alexei A Efros. Unsupervised visual representation learning by context prediction. In *Proceedings of the IEEE international conference on computer vision*, pages 1422–1430, 2015. 2, 3
- [19] Chengkai Hou, Jieyu Zhang, Haonan Wang, and Tianyi Zhou. Subclass-balancing contrastive learning for long-tailed recognition. *arXiv preprint arXiv:2306.15925*, 2023. 2, 3, 4
- [20] Mathilde Caron, Hugo Touvron, Ishan Misra, Hervé Jégou, Julien Mairal, Piotr Bojanowski, and Armand Joulin. Emerging properties in self-supervised vision transformers. In *Proceedings of the IEEE/CVF international conference on computer vision*, pages 9650–9660, 2021. 2, 3, 4, 8
- [21] Richard Zhang, Phillip Isola, and Alexei A Efros. Colorful image colorization. In *Computer Vision–ECCV 2016: 14th European Conference, Amsterdam, The Netherlands, October 11–14, 2016, Proceedings, Part III 14*, pages 649–666. Springer, 2016. 3
- [22] Deepak Pathak, Philipp Krahenbuhl, Jeff Donahue, Trevor Darrell, and Alexei A Efros. Context encoders: Feature learning by inpainting. In *Proceedings of the IEEE conference on computer vision and pattern recognition*, pages 2536–2544, 2016. 3

- [23] Richard Zhang, Phillip Isola, and Alexei A Efros. Split-brain autoencoders: Unsupervised learning by cross-channel prediction. In *Proceedings of the IEEE conference on computer vision and pattern recognition*, pages 1058–1067, 2017. 3
- [24] Aaron van den Oord, Yazhe Li, and Oriol Vinyals. Representation learning with contrastive predictive coding. *arXiv preprint arXiv:1807.03748*, 2018. 3, 4, 5, 8
- [25] Mathilde Caron, Ishan Misra, Julien Mairal, Priya Goyal, Piotr Bojanowski, and Armand Joulin. Unsupervised learning of visual features by contrasting cluster assignments. *Advances in neural information processing systems*, 33:9912–9924, 2020. 3, 4
- [26] Mark Chen, Alec Radford, Rewon Child, Jeffrey Wu, Heewoo Jun, David Luan, and Ilya Sutskever. Generative pretraining from pixels. In *International conference on machine learning*, pages 1691–1703. PMLR, 2020. 3, 4
- [27] Kaiping He, Haoqi Fan, Yuxin Wu, Saining Xie, and Ross Girshick. Momentum contrast for unsupervised visual representation learning. In *Proceedings of the IEEE/CVF conference on computer vision and pattern recognition*, pages 9729–9738, 2020. 3, 4, 8
- [28] Jean-Bastien Grill, Florian Strub, Florent Altché, Corentin Tallec, Pierre Richemond, Elena Buchatskaya, Carl Doersch, Bernardo Avila Pires, Zhaohan Guo, Mohammad Gheshlaghi Azar, et al. Bootstrap your own latent—a new approach to self-supervised learning. *Advances in neural information processing systems*, 33:21271–21284, 2020. 3, 4, 5, 6, 8
- [29] Zhenda Xie, Zheng Zhang, Yue Cao, Yutong Lin, Jianmin Bao, Zhuliang Yao, Qi Dai, and Han Hu. Simsim: A simple framework for masked image modeling. In *Proceedings of the IEEE/CVF Conference on Computer Vision and Pattern Recognition*, pages 9653–9663, 2022. 3, 4
- [30] Shaofeng Zhang, Feng Zhu, Rui Zhao, and Junchi Yan. Patch-level contrasting without patch correspondence for accurate and dense contrastive representation learning. *arXiv preprint arXiv:2306.13337*, 2023. 3, 4
- [31] Hsin-Ying Lee, Jia-Bin Huang, Maneesh Singh, and Ming-Hsuan Yang. Unsupervised representation learning by sorting sequences. In *Proceedings of the IEEE international conference on computer vision*, pages 667–676, 2017. 3
- [32] Himanshu Buckchash and Balasubramanian Raman. Sustained self-supervised pretraining for temporal order verification. In *Pattern Recognition and Machine Intelligence: 8th International Conference, PReMI 2019, Tezpur, India, December 17-20, 2019, Proceedings, Part I*, pages 140–149. Springer, 2019. 3
- [33] Himanshu Buckchash and Balasubramanian Raman. Dutrinet: dual-stream triplet siamese network for self-supervised action recognition by modeling temporal correlations. In *2020 IEEE 32nd International Conference on Tools with Artificial Intelligence (ICTAI)*, pages 488–495. IEEE, 2020. 3
- [34] Basura Fernando, Hakan Bilen, Efstratios Gavves, and Stephen Gould. Self-supervised video representation learning with odd-one-out networks. In *Proceedings of the IEEE conference on computer vision and pattern recognition*, pages 3636–3645, 2017. 3
- [35] Jinghao Zhou, Chen Wei, Huiyu Wang, Wei Shen, Cihang Xie, Alan Yuille, and Tao Kong. ibot: Image bert pre-training with online tokenizer. *arXiv preprint arXiv:2111.07832*, 2021. 4
- [36] Ishan Misra and Laurens van der Maaten. Self-supervised learning of pretext-invariant representations. In *Proceedings of the IEEE/CVF conference on computer vision and pattern recognition*, pages 6707–6717, 2020. 4
- [37] Jia Deng, Wei Dong, Richard Socher, Li-Jia Li, Kai Li, and Li Fei-Fei. Imagenet: A large-scale hierarchical image database. In *2009 IEEE conference on computer vision and pattern recognition*, pages 248–255. Ieee, 2009. 7
- [38] Adam Coates, Andrew Ng, and Honglak Lee. An analysis of single-layer networks in unsupervised feature learning. In *Proceedings of the fourteenth international conference on artificial intelligence and statistics*, pages 215–223. JMLR Workshop and Conference Proceedings, 2011. 7
- [39] Alex Krizhevsky, Geoffrey Hinton, et al. Learning multiple layers of features from tiny images. 2009. 7
- [40] Mohammed Ali Mnousta. Tiny imagenet, 2017. 7
- [41] Jiancheng Yang, Rui Shi, Donglai Wei, Zequan Liu, Lin Zhao, Bilian Ke, Hanspeter Pfister, and Bingbing Ni. Medmnist v2—a large-scale lightweight benchmark for 2d and 3d biomedical image classification. *Scientific Data*, 10(1):41, 2023. 8
- [42] Bastiaan S Veeling, Jasper Linmans, Jim Winkens, Taco Cohen, and Max Welling. Rotation equivariant cnns for digital pathology. In *Medical Image Computing and Computer Assisted Intervention—MICCAI 2018: 21st International Conference, Granada, Spain, September 16-20, 2018, Proceedings, Part II 11*, pages 210–218. Springer, 2018. 8

- [43] Adrien Bardes, Jean Ponce, and Yann Lecun. Vicreg: Variance-invariance-covariance regularization for self-supervised learning. In *ICLR 2022-International Conference on Learning Representations, 2022*. 10